Fermilab-Pub-08/097-E

Search for $t\bar{t}$ resonances in the lepton plus jets final state in $p\bar{p}$ collisions at $\sqrt{s} = 1.96$ TeV

V.M. Abazov[36], B. Abbott[75], M. Abolins[65], B.S. Acharya[29], M. Adams[51], T. Adams[49], E. Aguilo[6], S.H. Ahn[31], M. Ahsan[59], G.D. Alexeev[36], G. Alkhazov[40], A. Alton[64,a], G. Alverson[63], G.A. Alves[2], M. Anastasoaie[35], L.S. Ancu[35], T. Andeen[53], S. Anderson[45], B. Andrieu[17], M.S. Anzelc[53], M. Aoki[50], Y. Arnoud[14], M. Arov[60], M. Arthaud[18], A. Askew[49], B. Åsman[41], A.C.S. Assis Jesus[3], O. Atramentov[49], C. Avila[8], F. Badaud[13], A. Baden[61], L. Bagby[50], B. Baldin[50], D.V. Bandurin[59], P. Banerjee[29], S. Banerjee[29], E. Barberis[63], A.-F. Barfuss[15], P. Bargassa[80], P. Baringer[58], J. Barreto[2], J.F. Bartlett[50], U. Bassler[18], D. Bauer[43], S. Beale[6], A. Bean[58], M. Begalli[3], M. Begel[73], C. Belanger-Champagne[41], L. Bellantoni[50], A. Bellavance[50], J.A. Benitez[65], S.B. Beri[27], G. Bernardi[17], R. Bernhard[23], I. Bertram[42], M. Besançon[18], R. Beuselinck[43], V.A. Bezzubov[39], P.C. Bhat[50], V. Bhatnagar[27], C. Biscarat[20], G. Blazey[52], F. Blekman[43], S. Blessing[49], D. Bloch[19], K. Bloom[67], A. Boehnlein[50], D. Boline[62], T.A. Bolton[59], E.E. Boos[38], G. Borissov[42], T. Bose[77], A. Brandt[78], R. Brock[65], G. Brooijmans[70], A. Bross[50], D. Brown[81], N.J. Buchanan[49], D. Buchholz[53], M. Buehler[81], V. Buescher[22], V. Bunichev[38], S. Burdin[42,b], S. Burke[45], T.H. Burnett[82], C.P. Buszello[43], J.M. Butler[62], P. Calfayan[25], S. Calvet[16], J. Cammin[71], W. Carvalho[3], B.C.K. Casey[50], H. Castilla-Valdez[33], S. Chakrabarti[18], D. Chakraborty[52], K. Chan[6], K.M. Chan[55], A. Chandra[48], F. Charles[19,‡], E. Cheu[45], F. Chevallier[14], D.K. Cho[62], S. Choi[32], B. Choudhary[28], L. Christofek[77], T. Christoudias[43], S. Cihangir[50], D. Claes[67], J. Clutter[58], M. Cooke[80], W.E. Cooper[50], M. Corcoran[80], F. Couderc[18], M.-C. Cousinou[15], S. Crépé-Renaudin[14], D. Cutts[77], M. Ćwiok[30], H. da Motta[2], A. Das[45], G. Davies[43], K. De[78], S.J. de Jong[35], E. De La Cruz-Burelo[64], C. De Oliveira Martins[3], J.D. Degenhardt[64], F. Déliot[18], M. Demarteau[50], R. Demina[71], D. Denisov[50], S.P. Denisov[39], S. Desai[50], H.T. Diehl[50], M. Diesburg[50], A. Dominguez[67], H. Dong[72], L.V. Dudko[38], L. Duflot[16], S.R. Dugad[29], D. Duggan[49], A. Duperrin[15], J. Dyer[65], A. Dyshkant[52], M. Eads[67], D. Edmunds[65], J. Ellison[48], V.D. Elvira[50], Y. Enari[77], S. Eno[61], P. Ermolov[38], H. Evans[54], A. Evdokimov[73], V.N. Evdokimov[39], A.V. Ferapontov[59], T. Ferbel[71], F. Fiedler[24], F. Filthaut[35], W. Fisher[50], H.E. Fisk[50], M. Fortner[52], H. Fox[42], S. Fu[50], S. Fuess[50], T. Gadfort[70], C.F. Galea[35], E. Gallas[50], C. Garcia[71], A. Garcia-Bellido[82], V. Gavrilov[37], P. Gay[13], W. Geist[19], D. Gelé[19], C.E. Gerber[51], Y. Gershtein[49], D. Gillberg[6], G. Ginther[71], N. Gollub[41], B. Gómez[8], A. Goussiou[82], P.D. Grannis[72], H. Greenlee[50], Z.D. Greenwood[60], E.M. Gregores[4], G. Grenier[20], Ph. Gris[13], J.-F. Grivaz[16], A. Grohsjean[25], S. Grünendahl[50], M.W. Grünewald[30], F. Guo[72], J. Guo[72], G. Gutierrez[50], P. Gutierrez[75], A. Haas[70], N.J. Hadley[61], P. Haefner[25], S. Hagopian[49], J. Haley[68], I. Hall[65], R.E. Hall[47], L. Han[7], K. Harder[44], A. Harel[71], J.M. Hauptman[57], R. Hauser[65], J. Hays[43], T. Hebbeker[21], D. Hedin[52], J.G. Hegeman[34], A.P. Heinson[48], U. Heintz[62], C. Hensel[22,d], K. Herner[72], G. Hesketh[63], M.D. Hildreth[55], R. Hirosky[81], J.D. Hobbs[72], B. Hoeneisen[12], H. Hoeth[26], M. Hohlfeld[22], S.J. Hong[31], S. Hossain[75], P. Houben[34], Y. Hu[72], Z. Hubacek[10], V. Hynek[9], I. Iashvili[69], R. Illingworth[50], A.S. Ito[50], S. Jabeen[62], M. Jaffré[16], S. Jain[75], K. Jakobs[23], C. Jarvis[61], R. Jesik[43], K. Johns[45], C. Johnson[70], M. Johnson[50], A. Jonckheere[50], P. Jonsson[43], A. Juste[50], E. Kajfasz[15], J.M. Kalk[60], D. Karmanov[38], P.A. Kasper[50], I. Katsanos[70], D. Kau[49], V. Kaushik[78], R. Kehoe[79], S. Kermiche[15], N. Khalatyan[50], A. Khanov[76], A. Kharchilava[69], Y.M. Kharzheev[36], D. Khatidze[70], T.J. Kim[31], M.H. Kirby[53], M. Kirsch[21], B. Klima[50], J.M. Kohli[27], J.-P. Konrath[23], A.V. Kozelov[39], J. Kraus[65], D. Krop[54], T. Kuhl[24], A. Kumar[69], A. Kupco[11], T. Kurča[20], V.A. Kuzmin[38], J. Kvita[9], F. Lacroix[13], D. Lam[55], S. Lammers[70], G. Landsberg[77], P. Lebrun[20], W.M. Lee[50], A. Leflat[38], J. Lellouch[17], J. Leveque[45], J. Li[78], L. Li[48], Q.Z. Li[50], S.M. Lietti[5], J.G.R. Lima[52], D. Lincoln[50], J. Linnemann[65], V.V. Lipaev[39], R. Lipton[50], Y. Liu[7], Z. Liu[6], A. Lobodenko[40], M. Lokajicek[11], P. Love[42], H.J. Lubatti[82], R. Luna[3], A.L. Lyon[50], A.K.A. Maciel[2], D. Mackin[80], R.J. Madaras[46], P. Mättig[26], C. Magass[21], A. Magerkurth[64], P.K. Mal[82], H.B. Malbouisson[3], S. Malik[67], V.L. Malyshev[36], H.S. Mao[50], Y. Maravin[59], B. Martin[14], R. McCarthy[72], A. Melnitchouk[66], L. Mendoza[8], P.G. Mercadante[5], M. Merkin[38], K.W. Merritt[50], A. Meyer[21], J. Meyer[22,d], T. Millet[20], J. Mitrevski[70], R.K. Mommsen[44], N.K. Mondal[29], R.W. Moore[6], T. Moulik[58], G.S. Muanza[20], M. Mulhearn[70], O. Mundal[22], L. Mundim[3], E. Nagy[15], M. Naimuddin[50], M. Narain[77], N.A. Naumann[35], H.A. Neal[64], J.P. Negret[8], P. Neustroev[40], H. Nilsen[23], H. Nogima[3], S.F. Novaes[5], T. Nunnemann[25], V. O'Dell[50], D.C. O'Neil[6], G. Obrant[40], C. Ochando[16], D. Onoprienko[59], N. Oshima[50], N. Osman[43], J. Osta[55], R. Otec[10], G.J. Otero y Garzón[50], M. Owen[44], P. Padley[80], M. Pangilinan[77], N. Parashar[56], S.-J. Park[22,d], S.K. Park[31], J. Parsons[70], R. Partridge[77], N. Parua[54], A. Patwa[73],

G. Pawloski[80], B. Penning[23], M. Perfilov[38], K. Peters[44], Y. Peters[26], P. Pétroff[16], M. Petteni[43], R. Piegaia[1], J. Piper[65], M.-A. Pleier[22], P.L.M. Podesta-Lerma[33,c], V.M. Podstavkov[50], Y. Pogorelov[55], M.-E. Pol[2], P. Polozov[37], B.G. Pope[65], A.V. Popov[39], C. Potter[6], W.L. Prado da Silva[3], H.B. Prosper[49], S. Protopopescu[73], J. Qian[64], A. Quadt[22,d], B. Quinn[66], A. Rakitine[42], M.S. Rangel[2], K. Ranjan[28], P.N. Ratoff[42], P. Renkel[79], S. Reucroft[63], P. Rich[44], J. Rieger[54], M. Rijssenbeek[72], I. Ripp-Baudot[19], F. Rizatdinova[76], S. Robinson[43], R.F. Rodrigues[3], M. Rominsky[75], C. Royon[18], P. Rubinov[50], R. Ruchti[55], G. Safronov[37], G. Sajot[14], A. Sánchez-Hernández[33], M.P. Sanders[17], B. Sanghi[50], A. Santoro[3], G. Savage[50], L. Sawyer[60], T. Scanlon[43], D. Schaile[25], R.D. Schamberger[72], Y. Scheglov[40], H. Schellman[53], T. Schliephake[26], C. Schwanenberger[44], A. Schwartzman[68], R. Schwienhorst[65], J. Sekaric[49], H. Severini[75], E. Shabalina[51], M. Shamim[59], V. Shary[18], A.A. Shchukin[39], R.K. Shivpuri[28], V. Siccardi[19], V. Simak[10], V. Sirotenko[50], P. Skubic[75], P. Slattery[71], D. Smirnov[55], G.R. Snow[67], J. Snow[74], S. Snyder[73], S. Söldner-Rembold[44], L. Sonnenschein[17], A. Sopczak[42], M. Sosebee[78], K. Soustruznik[9], B. Spurlock[78], J. Stark[14], J. Steele[60], V. Stolin[37], D.A. Stoyanova[39], J. Strandberg[64], S. Strandberg[41], M.A. Strang[69], E. Strauss[72], M. Strauss[75], R. Ströhmer[25], D. Strom[53], L. Stutte[50], S. Sumowidagdo[49], P. Svoisky[55], A. Sznajder[3], P. Tamburello[45], A. Tanasijczuk[1], W. Taylor[6], J. Temple[45], B. Tiller[25], F. Tissandier[13], M. Titov[18], V.V. Tokmenin[36], T. Toole[61], I. Torchiani[23], T. Trefzger[24], D. Tsybychev[72], B. Tuchming[18], C. Tully[68], P.M. Tuts[70], R. Unalan[65], L. Uvarov[40], S. Uvarov[40], S. Uzunyan[52], B. Vachon[6], P.J. van den Berg[34], R. Van Kooten[54], W.M. van Leeuwen[34], N. Varelas[51], E.W. Varnes[45], I.A. Vasilyev[39], M. Vaupel[26], P. Verdier[20], L.S. Vertogradov[36], M. Verzocchi[50], F. Villeneuve-Seguier[43], P. Vint[43], P. Vokac[10], E. Von Toerne[59], M. Voutilainen[68,e], R. Wagner[68], H.D. Wahl[49], L. Wang[61], M.H.L.S. Wang[50], J. Warchol[55], G. Watts[82], M. Wayne[55], G. Weber[24], M. Weber[50], L. Welty-Rieger[54], A. Wenger[23,f], N. Wermes[22], M. Wetstein[61], A. White[78], D. Wicke[26], G.W. Wilson[58], S.J. Wimpenny[48], M. Wobisch[60], D.R. Wood[63], T.R. Wyatt[44], Y. Xie[77], S. Yacoob[53], R. Yamada[50], M. Yan[61], T. Yasuda[50], Y.A. Yatsunenko[36], K. Yip[73], H.D. Yoo[77], S.W. Youn[53], J. Yu[78], C. Zeitnitz[26], T. Zhao[82], B. Zhou[64], J. Zhu[72], M. Zielinski[71], D. Zieminska[54], A. Zieminski[54,‡], L. Zivkovic[70], V. Zutshi[52], and E.G. Zverev[38]

(The DØ Collaboration)

[1]*Universidad de Buenos Aires, Buenos Aires, Argentina*
[2]*LAFEX, Centro Brasileiro de Pesquisas Físicas, Rio de Janeiro, Brazil*
[3]*Universidade do Estado do Rio de Janeiro, Rio de Janeiro, Brazil*
[4]*Universidade Federal do ABC, Santo André, Brazil*
[5]*Instituto de Física Teórica, Universidade Estadual Paulista, São Paulo, Brazil*
[6]*University of Alberta, Edmonton, Alberta, Canada, Simon Fraser University, Burnaby, British Columbia, Canada, York University, Toronto, Ontario, Canada, and McGill University, Montreal, Quebec, Canada*
[7]*University of Science and Technology of China, Hefei, People's Republic of China*
[8]*Universidad de los Andes, Bogotá, Colombia*
[9]*Center for Particle Physics, Charles University, Prague, Czech Republic*
[10]*Czech Technical University, Prague, Czech Republic*
[11]*Center for Particle Physics, Institute of Physics, Academy of Sciences of the Czech Republic, Prague, Czech Republic*
[12]*Universidad San Francisco de Quito, Quito, Ecuador*
[13]*LPC, Univ Blaise Pascal, CNRS/IN2P3, Clermont, France*
[14]*LPSC, Université Joseph Fourier Grenoble 1, CNRS/IN2P3, Institut National Polytechnique de Grenoble, France*
[15]*CPPM, Aix-Marseille Université, CNRS/IN2P3, Marseille, France*
[16]*LAL, Univ Paris-Sud, IN2P3/CNRS, Orsay, France*
[17]*LPNHE, IN2P3/CNRS, Universités Paris VI and VII, Paris, France*
[18]*DAPNIA/Service de Physique des Particules, CEA, Saclay, France*
[19]*IPHC, Université Louis Pasteur et Université de Haute Alsace, CNRS/IN2P3, Strasbourg, France*
[20]*IPNL, Université Lyon 1, CNRS/IN2P3, Villeurbanne, France and Université de Lyon, Lyon, France*
[21]*III. Physikalisches Institut A, RWTH Aachen, Aachen, Germany*
[22]*Physikalisches Institut, Universität Bonn, Bonn, Germany*
[23]*Physikalisches Institut, Universität Freiburg, Freiburg, Germany*
[24]*Institut für Physik, Universität Mainz, Mainz, Germany*
[25]*Ludwig-Maximilians-Universität München, München, Germany*
[26]*Fachbereich Physik, University of Wuppertal, Wuppertal, Germany*
[27]*Panjab University, Chandigarh, India*
[28]*Delhi University, Delhi, India*

[29]*Tata Institute of Fundamental Research, Mumbai, India*
[30]*University College Dublin, Dublin, Ireland*
[31]*Korea Detector Laboratory, Korea University, Seoul, Korea*
[32]*SungKyunKwan University, Suwon, Korea*
[33]*CINVESTAV, Mexico City, Mexico*
[34]*FOM-Institute NIKHEF and University of Amsterdam/NIKHEF, Amsterdam, The Netherlands*
[35]*Radboud University Nijmegen/NIKHEF, Nijmegen, The Netherlands*
[36]*Joint Institute for Nuclear Research, Dubna, Russia*
[37]*Institute for Theoretical and Experimental Physics, Moscow, Russia*
[38]*Moscow State University, Moscow, Russia*
[39]*Institute for High Energy Physics, Protvino, Russia*
[40]*Petersburg Nuclear Physics Institute, St. Petersburg, Russia*
[41]*Lund University, Lund, Sweden, Royal Institute of Technology and Stockholm University, Stockholm, Sweden, and Uppsala University, Uppsala, Sweden*
[42]*Lancaster University, Lancaster, United Kingdom*
[43]*Imperial College, London, United Kingdom*
[44]*University of Manchester, Manchester, United Kingdom*
[45]*University of Arizona, Tucson, Arizona 85721, USA*
[46]*Lawrence Berkeley National Laboratory and University of California, Berkeley, California 94720, USA*
[47]*California State University, Fresno, California 93740, USA*
[48]*University of California, Riverside, California 92521, USA*
[49]*Florida State University, Tallahassee, Florida 32306, USA*
[50]*Fermi National Accelerator Laboratory, Batavia, Illinois 60510, USA*
[51]*University of Illinois at Chicago, Chicago, Illinois 60607, USA*
[52]*Northern Illinois University, DeKalb, Illinois 60115, USA*
[53]*Northwestern University, Evanston, Illinois 60208, USA*
[54]*Indiana University, Bloomington, Indiana 47405, USA*
[55]*University of Notre Dame, Notre Dame, Indiana 46556, USA*
[56]*Purdue University Calumet, Hammond, Indiana 46323, USA*
[57]*Iowa State University, Ames, Iowa 50011, USA*
[58]*University of Kansas, Lawrence, Kansas 66045, USA*
[59]*Kansas State University, Manhattan, Kansas 66506, USA*
[60]*Louisiana Tech University, Ruston, Louisiana 71272, USA*
[61]*University of Maryland, College Park, Maryland 20742, USA*
[62]*Boston University, Boston, Massachusetts 02215, USA*
[63]*Northeastern University, Boston, Massachusetts 02115, USA*
[64]*University of Michigan, Ann Arbor, Michigan 48109, USA*
[65]*Michigan State University, East Lansing, Michigan 48824, USA*
[66]*University of Mississippi, University, Mississippi 38677, USA*
[67]*University of Nebraska, Lincoln, Nebraska 68588, USA*
[68]*Princeton University, Princeton, New Jersey 08544, USA*
[69]*State University of New York, Buffalo, New York 14260, USA*
[70]*Columbia University, New York, New York 10027, USA*
[71]*University of Rochester, Rochester, New York 14627, USA*
[72]*State University of New York, Stony Brook, New York 11794, USA*
[73]*Brookhaven National Laboratory, Upton, New York 11973, USA*
[74]*Langston University, Langston, Oklahoma 73050, USA*
[75]*University of Oklahoma, Norman, Oklahoma 73019, USA*
[76]*Oklahoma State University, Stillwater, Oklahoma 74078, USA*
[77]*Brown University, Providence, Rhode Island 02912, USA*
[78]*University of Texas, Arlington, Texas 76019, USA*
[79]*Southern Methodist University, Dallas, Texas 75275, USA*
[80]*Rice University, Houston, Texas 77005, USA*
[81]*University of Virginia, Charlottesville, Virginia 22901, USA and*
[82]*University of Washington, Seattle, Washington 98195, USA*

(Dated: April 23, 2008)

We present a search for a narrow-width heavy resonance decaying into top quark pairs ($X \to t\bar{t}$) in $p\bar{p}$ collisions at $\sqrt{s} = 1.96\,\mathrm{TeV}$ using approximately $0.9\,\mathrm{fb}^{-1}$ of data collected with the D0 detector at the Fermilab Tevatron Collider. This analysis considers $t\bar{t}$ candidate events in the lepton plus jets channel with at least one identified b jet and uses the $t\bar{t}$ invariant mass distribution to search for evidence of resonant production. We find no evidence for a narrow resonance X decaying to $t\bar{t}$. Therefore, we set upper limits on $\sigma_X \cdot B(X \to t\bar{t})$ for different hypothesized resonance masses using a Bayesian approach. For a Topcolor-assisted technicolor model, the existence of a leptophobic Z'

boson with mass $M_{Z'} < 700\,\mathrm{GeV}$ and width $\Gamma_{Z'} = 0.012 M_{Z'}$ can be excluded at the 95% C.L.

PACS numbers: 14.65.Ha, 14.70.Pw

INTRODUCTION

The top quark has by far the largest mass of all the known fermions. Unknown heavy resonances may play a role in the production of top quark pairs ($t\bar{t}$) and add a resonant part to the standard model (SM) production mechanism mediated by the strong interaction. Such resonant production is possible for massive Z-like bosons in extended gauge theories [1], Kaluza-Klein states of the gluon or Z boson [2, 3], axigluons [4], Topcolor [5], and other theories beyond the SM. Independent of the exact model, resonant production of top quark pairs could be visible in the reconstructed $t\bar{t}$ invariant mass distribution.

In this Letter, we present a search for a narrow-width heavy resonance X decaying into $t\bar{t}$. We consider the lepton+jets (ℓ+jets, where $\ell = e$ or μ) final state. The event signature is one isolated electron or muon with high momentum transverse to the beam axis (p_T), large transverse energy imbalance ($\not\!\!E_T$) due to the undetected neutrino, and at least four jets, two of which result from the hadronization of b quarks. The analyzed dataset corresponds to an integrated luminosity of $913 \pm 56\,\mathrm{pb}^{-1}$ in the e+jets channel and $871 \pm 53\,\mathrm{pb}^{-1}$ in the μ+jets channel, collected with the D0 detector between August 2002 and December 2005. The analysis uses events with at least three reconstructed jets. Backgrounds from light-quarks are further reduced by identifying b jets. After b tagging, the dominant physics background for a resonance signal is non-resonant SM $t\bar{t}$ production. Smaller contributions arise from the direct production of W bosons in association with jets (W+jets), as well as instrumental background originating from multijet processes with jets faking isolated leptons. The search for resonant production in the $t\bar{t}$ invariant mass distribution is performed using Bayesian statistics to compare SM and resonant production to the observed mass distribution.

Previous searches performed by the CDF and D0 collaborations in Run I found no evidence for a $t\bar{t}$ resonance [6, 7]. In these studies, a Topcolor model was used as a reference to quote mass limits. According to this model [5], a large top quark mass can be generated through the formation of a dynamical $t\bar{t}$ condensate, Z', due to a new strong gauge force with large coupling to the third generation of fermions. In one particular model, Topcolor-assisted technicolor [8], the Z' boson has large couplings only to the first and third generation of quarks and has no significant couplings to leptons. Limits obtained on $\sigma_X \cdot B(X \to t\bar{t})$ are used to set a lower bound on the mass of such a leptophobic Z' boson. In Run I CDF found $M_{Z'} > 480\,\mathrm{GeV}$ with $106\,\mathrm{pb}^{-1}$ of data [6], and D0 obtained $M_{Z'} > 560\,\mathrm{GeV}$ using $130\,\mathrm{pb}^{-1}$ [7], both at the 95% C.L. and for a resonance with width $\Gamma_{Z'} = 0.012 M_{Z'}$.

D0 DETECTOR

The D0 detector [9] has a central-tracking system consisting of a silicon microstrip tracker and a central fiber tracker, both located within a 2 T superconducting solenoidal magnet, with designs optimized for tracking and vertexing at pseudorapidities $|\eta| < 3$ and $|\eta| < 2.5$, respectively. The pseudorapidity, η, is defined with respect to the beam axis. Central and forward preshower detectors are positioned just outside of the superconducting coil. A liquid-argon and uranium calorimeter has a central section (CC) covering pseudorapidities $|\eta| \lesssim 1.1$, and two end calorimeters (EC) that extend coverage to $|\eta| \approx 4.2$, with all three housed in separate cryostats [10]. An outer muon system covering $|\eta| < 2$ consists of a layer of tracking detectors and scintillation trigger counters in front of 1.8 T iron toroids, followed by two similar layers after the toroids [11]. Luminosity is measured using plastic scintillator arrays placed in front of the EC cryostats. The three-level trigger and data acquisition systems are designed to accommodate the high luminosities of Run II and record events of interest at up to about 100 Hz.

EVENT SELECTION

To select top quark pair candidates in the e+jets and μ+jets decay channels, triggers that required a jet and an electron or muon are used. The event selection requires either an isolated electron with $p_T > 20\,\mathrm{GeV}$ and $|\eta| < 1.1$, or an isolated muon with $p_T > 20\,\mathrm{GeV}$ and $|\eta| < 2.0$. No additional isolated leptons with $p_T > 15\,\mathrm{GeV}$ are allowed in the event. Details of the lepton identification and isolation criteria are described in [12, 13]. We require $\not\!\!E_T$ to exceed 20 GeV (25 GeV) for the e+jets (μ+jets) channel. Jets are defined using a cone algorithm [14] with radius $\mathcal{R}_{\mathrm{cone}} = 0.5$, where $\mathcal{R}_{\mathrm{cone}} = \sqrt{(\Delta\phi)^2 + (\Delta y)^2}$, ϕ is the azimuthal angle, and y the rapidity. The selected events must contain three or more jets with $p_T > 20\,\mathrm{GeV}$ and $|y| < 2.5$. At least one of the jets is required to have $p_T > 40\,\mathrm{GeV}$. Events with mismeasured lepton momentum are rejected by requiring the $\not\!\!E_T$ to be acollinear with the lepton direction in the transverse plane: $\Delta\phi(e, \not\!\!E_T) > 2.2 - 0.045\,\mathrm{GeV}^{-1}\,\not\!\!E_T$ and $\Delta\phi(\mu, \not\!\!E_T) > 2.1 - 0.035\,\mathrm{GeV}^{-1}\,\not\!\!E_T$ [15].

To improve the signal-to-background ratio, at least one jet is required to be identified as a b jet. The tagging algorithm uses the impact parameters of tracks matched

to a given jet and information on vertex mass, the decay length significance, and the number of participating tracks for any reconstructed secondary vertex within the cone of the given jet. The information is combined in a neural network to obtain the output variable, NN_B, which tends towards one for b jets and towards zero for light quark jets [16]. In this analysis we consider jets to be b-tagged if $\mathrm{NN}_B > 0.65$ which corresponds to a tagging efficiency for b jets of about 55% with a tagging rate for light quark jets of less than 1%.

We independently analyze events with three and four or more jets and separate singly tagged and doubly tagged events, since the channels have different signal-to-background ratios and systematic uncertainties.

SIGNAL AND BACKGROUND MODELING

Simulated events are used to determine selection efficiencies for the resonant $t\bar{t}$ production signal and for background sources except those in which instrumental effects give fake leptons and $\not\!\!E_T$ in multijet production events. Samples of resonant $t\bar{t}$ production are generated with PYTHIA [17] for ten different choices of the resonance mass M_X between 350 GeV and 1 TeV. In all cases, the width of the resonance is set to $\Gamma_X = 0.012 M_X$. This qualifies the X boson as a narrow resonance since its width is smaller than the estimated mass resolution of the D0 detector of 5–10%. The generated resonance is forced to decay into $t\bar{t}$.

Standard model $t\bar{t}$ and diboson backgrounds (WW, WZ, and ZZ) are generated with PYTHIA [17]. Single top quark production is generated using the COMPHEP generator [18]. A top quark mass of 175 GeV is used for both resonant and SM top production processes. W+jets and Z+jets events are generated using ALPGEN [19] to model the hard interaction and PYTHIA for parton showering, hadronization and hadron decays. To avoid double counting between the hard matrix element and the parton shower, the MLM jet-matching algorithm is used [20]. The CTEQ6L1 parton distribution functions [21, 22] are used for all samples. The generated events are processed through the full GEANT3-based [23] simulation of the D0 detector and the same reconstruction program as used for data.

The SM $t\bar{t}$, single top quark, diboson, and Z+jets backgrounds are estimated completely from Monte Carlo (MC) simulation, to obtain the total acceptance as well as the shape of the reconstructed $t\bar{t}$ invariant mass distribution. Trigger inefficiencies and differences between data and MC lepton and jet identification efficiencies are accounted for by weighting the simulated events [15]. Jet b-tagging probabilities are measured in data and parametrized as functions of p_T and η. They are used to weight each simulated event according to its event b-tagging probability. Finally, the expected yields are normalized to the SM theoretical prediction. A $t\bar{t}$ production of $\sigma_{t\bar{t}} = 6.77 \pm 0.60$ pb for $m_t = 175$ GeV [24] is used. Z+jets, single top quark and diboson samples are normalized to their next-to-leading-order cross sections [25–27].

TABLE I: Event yields for the expected SM background and for data. The uncertainties are statistical and systematic.

	3 jets	≥ 4 jets
$t\bar{t}$	167.4	160.5
W+jets	118.2	24.1
Other MC	34.8	9.8
Multijet	31.3	7.4
Total background	351.7 ± 29.3	201.8 ± 29.0
Data	370	237

The W+jets background is estimated from a combination of data and MC information. The expected number of W+jets events in the b-tagged sample is computed as the product of the estimated number of W+jets before b tagging and the expected event b-tagging probability. The former is obtained from the observed number of events with real leptons in data, computed using the matrix method [12], and then subtracting the expected contribution from other SM production processes. The b-tagging probability is obtained by combining the W+jets flavor fractions estimated from MC with the event b-tagging probability, estimated from b tag rate functions. The shape of the reconstructed invariant mass distribution is obtained from the MC simulation.

The multijet background is completely determined from data. The total number of expected events is estimated by applying the matrix method to the each of the b-tagged subsamples. The shape is derived from events with leptons failing the isolation requirements. A summary of the prediction for the different background contributions in the combined ℓ+jets channels, along with the observed number of events in data, is given in Table I. Systematic uncertainties are discussed below.

RECONSTRUCTION OF THE $t\bar{t}$ INVARIANT MASS DISTRIBUTION

The $t\bar{t}$ invariant mass is reconstructed from the four-momenta of up to the four highest p_T jets, the lepton momentum, and the neutrino momentum. The latter is obtained from the transverse missing energy and a W-mass constraint. The neutrino transverse momentum is identified with the missing transverse momentum, given by $\not\!\!E_T$ and its direction. The neutrino momentum along the beam direction, p_z^ν, is estimated by solving the equation $M_W^2 = (p^\ell + p^\nu)^2$, where p^ℓ (p^ν) is the lepton (neutrino) four momentum. If there are two solutions, the one with the smaller $|p_z^\nu|$ is taken; if no solution exists, p_z^ν is set to zero. This method gives better sensitivity for high mass

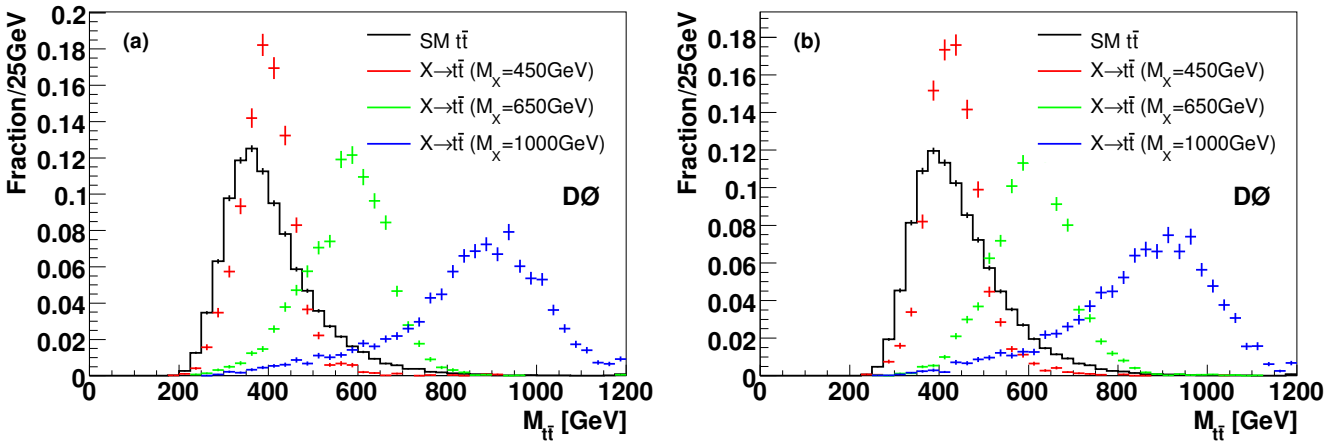

FIG. 1: Shape comparison of the expected $t\bar{t}$ invariant mass distributions for SM top quark pair production (histogram) and resonant production from narrow-width resonances of mass M_X = 450, 650, and 1000 GeV, for (a) 3 jets events and (b) $\geq$ 4 jets events.

resonances than a previously applied constrained kinematic fit technique [7], while only slightly reducing the sensitivity for lower resonance masses. Moreover, this direct reconstruction allows the inclusion of data with fewer than four jets in the case that some jets are merged, further increasing the sensitivity. The expected $t\bar{t}$ invariant mass distributions for three different resonance masses are compared to the SM expectation in Fig. 1.

SYSTEMATIC UNCERTAINTIES

The systematic uncertainties can be classified as those affecting only normalization and those affecting the shape of any of the signal or background invariant mass distributions. The systematic uncertainties affecting only the normalization include the theoretical uncertainty on the SM prediction for $\sigma_{t\bar{t}}$ (9%), the uncertainty on the integrated luminosity (6.1%) [28], and the uncertainty on the lepton identification efficiencies.

The systematic uncertainties affecting the shape of the invariant mass distribution as well as the normalization are studied in signal and background samples. These include uncertainties on the jet energy calibration, jet reconstruction efficiency, and b-tagging parameterizations for b, c and light jets. The effect due to the top quark mass uncertainty is computed by changing m_t in the simulation of $t\bar{t}$ to 165 GeV and 185 GeV, normalized to their corresponding theoretical cross sections. The effect is scaled to correspond to a top quark mass uncertainty of $\pm$5 GeV. The difference in the $t\bar{t}$ acceptance due to the top quark mass variation is also included in the systematic uncertainty.

The fraction of heavy flavor in the W+jets background is measured in control samples, and a corresponding uncertainty on the W+jets flavor composition is used. Also the uncertainties on the b-fragmentation and the uncertainties of the efficiencies used in the matrix method are taken into account.

Table II gives a summary of the relative systematic uncertainties on the total SM background normalization for the combined ℓ+jets channels. The effect of the different systematic uncertainties on the shape of the $t\bar{t}$ invariant mass distribution cannot be inferred from this table, but is included in the analysis.

RESULT

After all selection cuts, 319 events remain in the e+jets channel and 288 events in the μ+jets channel. The sums of all SM and multijet instrumental backgrounds are

TABLE II: The relative systematic uncertainties on the overall normalization of the SM background and for a resonance mass of M_X = 650 GeV, with at least one b-tagged jet. The uncertainties shown are symmetrized. The actual asymmetric uncertainties and the effect of shape-changing systematic errors are used in the limit setting.

Source	SM processes (backgrounds)		Resonance M_X = 650 GeV	
	3 jets	$\geq$ 4 jets	3 jets	$\geq$ 4 jets
Jet energy calibration	$\pm$1.0%	$\pm$5.8%	$\pm$3.7%	$\pm$5.5%
Jet energy resolution	$\pm$0.2%	$<$ 0.1%	$\pm$1.2%	$\pm$0.2%
Jet identification	$\pm$0.6%	$\pm$2.0%	$\pm$0.6%	$\pm$1.6%
$\sigma_{t\bar{t}}(m_t = 175\,\text{GeV})$	$\pm$3.1%	$\pm$5.9%	–	–
Top quark mass	$\pm$5.2%	$\pm$6.9%	–	–
b tagging	$\pm$3.1%	$\pm$4.9%	$\pm$3.9%	$\pm$3.6%
b fragmentation	$\pm$0.3%	$\pm$0.4%	$\pm$0.6%	$\pm$0.6%
W+jets (heavy flavor)	$\pm$2.5%	$\pm$0.9%	–	–
Multijet lepton fake rate	$\pm$0.3%	$<$ 0.1%	–	–
Selection efficiencies	$\pm$3.1%	$\pm$5.3%	$\pm$3.6%	$\pm$3.6%
Luminosity	$\pm$2.6%	$\pm$4.2%	$\pm$6.1%	$\pm$6.1%

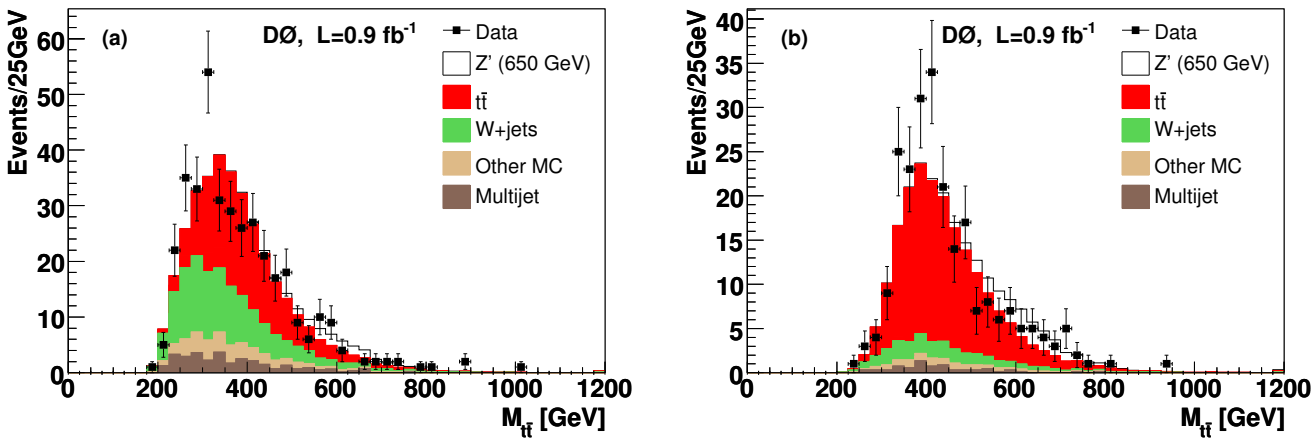

FIG. 2: Expected and observed $t\bar{t}$ invariant mass distribution for the combined (a) $\ell+3$ jets and (b) $\ell+4$ or more jets channels, with at least one identified b jet. Errors shown on the data points are statistical. Superimposed as white area is the expected signal for a Topcolor-assisted technicolor Z' boson with $M_{Z'} = 650\,\text{GeV}$.

303 ± 22 and 251 ± 19 events, respectively. Invariant mass distributions are computed for events with exactly one b tag and for events with more than one b tag. Additionally, the distributions are separated into 3 jets and ≥ 4 jets samples. The measured invariant mass distributions and corresponding background estimations are shown in Fig. 2 for the 3 jets and ≥ 4 jets samples.

Finding no significant deviation from the SM expectation, we apply a Bayesian approach to calculate 95% C.L. upper limits on $\sigma_X \cdot B(X \to t\bar{t})$ for hypothesized values of M_X between 350 and 1000 GeV. A Poisson distribution is assumed for the number of observed events in each bin, and flat prior probabilities are taken for the signal cross section times branching fraction. The prior for the combined signal acceptance and background yields is a multivariate Gaussian with uncertainties and correlations described by a covariance matrix [29].

The expected and observed 95% C.L. upper limits on $\sigma_X \cdot B(X \to t\bar{t})$ as a function of M_X, after combining the 1 and 2 b-tag samples and the 3 and ≥ 4 jets samples, are summarized in Table III and displayed in Fig. 3. This figure also includes the predicted $\sigma_X \cdot B(X \to t\bar{t})$ for a leptophobic Z' boson with $\Gamma_{Z'} = 0.012 M_{Z'}$ computed using CTEQ6L1 parton distribution functions. The comparison of the observed cross section limits with the Z' boson prediction excludes $M_{Z'} < 700\,\text{GeV}$ at the 95% C.L. Due to a small excess of data over expectation (of no more than 1.5σ significance) for invariant masses in the range between 600 and 700 GeV, the observed limits do not reach the expected limit for a Z' boson of 780 GeV.

TABLE III: Expected and observed limits for $\sigma_X \cdot B(X \to t\bar{t})$ at the 95% C.L. when combining all channels and taking all systematic uncertainties into account.

M_X [GeV]	Exp. limit [pb]	Obs. limit [pb]
350	2.08	3.19
400	2.09	2.32
450	1.59	1.59
500	1.24	0.99
550	0.94	0.80
600	0.68	0.79
650	0.55	0.87
750	0.36	0.66
850	0.28	0.49
1000	0.22	0.36

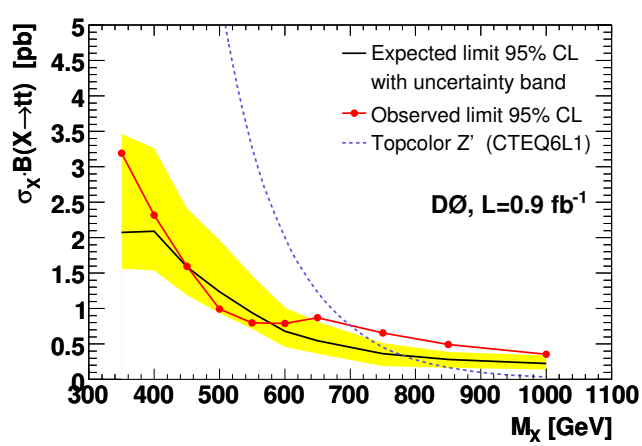

FIG. 3: Expected and observed 95% C.L. upper limits on $\sigma_X \cdot B(X \to t\bar{t})$ compared with the predicted Topcolor-assisted technicolor cross section for a Z' boson with a width of $\Gamma_{Z'} = 0.012 M_{Z'}$ as a function of resonance mass M_X. The shaded band gives the ± 1 sigma uncertainty in the SM expected limit.

CONCLUSION

A search for a narrow-width heavy resonance decaying to $t\bar{t}$ in the ℓ+jets final states has been performed using data corresponding to an integrated luminosity of about $0.9\,\mathrm{fb}^{-1}$, collected with the D0 detector at the Tevatron collider. By analyzing the reconstructed $t\bar{t}$ invariant mass distribution and using a Bayesian method, model independent upper limits on $\sigma_X \cdot B(X \to t\bar{t})$ have been obtained for different hypothesized masses of a narrow-width heavy resonance decaying into $t\bar{t}$. Within a Topcolor-assisted technicolor model, the existence of a leptophobic Z' boson with $M_{Z'} < 700\,\mathrm{GeV}$ and width $\Gamma_{Z'} = 0.012 M_{Z'}$ is excluded at the 95% C.L.

We thank the staffs at Fermilab and collaborating institutions, and acknowledge support from the DOE and NSF (USA); CEA and CNRS/IN2P3 (France); FASI, Rosatom and RFBR (Russia); CNPq, FAPERJ, FAPESP and FUNDUNESP (Brazil); DAE and DST (India); Colciencias (Colombia); CONACyT (Mexico); KRF and KOSEF (Korea); CONICET and UBACyT (Argentina); FOM (The Netherlands); STFC (United Kingdom); MSMT and GACR (Czech Republic); CRC Program, CFI, NSERC and WestGrid Project (Canada); BMBF and DFG (Germany); SFI (Ireland); The Swedish Research Council (Sweden); CAS and CNSF (China); and the Alexander von Humboldt Foundation.

[a] Visitor from Augustana College, Sioux Falls, SD, USA.
[b] Visitor from The University of Liverpool, Liverpool, UK.
[c] Visitor from ICN-UNAM, Mexico City, Mexico.
[d] Visitor from II. Physikalisches Institut, Georg-August-University, Göttingen, Germany.
[e] Visitor from Helsinki Institute of Physics, Helsinki, Finland.
[f] Visitor from Universität Zürich, Zürich, Switzerland.
[‡] Deceased.

[1] A. Leike, Phys. Rept. 317 (1999) 143.
[2] B. Lillie, L. Randall, and L.-T. Wang, JHEP 09 (2007) 074.
[3] T. G. Rizzo, Phys. Rev. D 61 (2000) 055005.
[4] L. M. Sehgal and M. Wanninger, Phys. Lett. B 200 (1988) 211.
[5] C. T. Hill and S. Parke, Phys. Rev. D 49 (1994) 4454.
[6] CDF Collaboration, T. Affolder et al., Phys. Rev. Lett. 85 (2000) 2062.
[7] D0 Collaboration, V. M. Abazov et al., Phys. Rev. Lett. 92 (2004) 221801.
[8] R. M. Harris, C. T. Hill, and S. Parke, `arXiv:hep-ph/9911288` (1999).
[9] D0 Collaboration, V. M. Abazov et al., Nucl. Instrum. Meth. Phys. Res. A 565 (2006) 463.
[10] D0 Collaboration, S. Abachi et al., Nucl. Instrum. Meth. Phys. Res. A 338 (1994) 185.
[11] V. M. Abazov et al., Nucl. Instrum. Meth. Phys. Res. A 552 (2005) 372.
[12] D0 Collaboration, V. M. Abazov et al., Phys. Lett. B 626 (2005) 45.
[13] D0 Collaboration, V. M. Abazov et al., Phys. Lett. B 626 (2005) 35.
[14] G. Blazey et al., in "QCD and weak boson physics in Run II", U. Baur, R. K. Ellis, and D. Zeppenfeld, Eds., FERMILAB-PUB-00-297, (2000).
[15] D0 Collaboration, V. M. Abazov et al., Phys. Rev. D 76 (2007) 092007.
[16] T. Scanlon, FERMILAB-THESIS-2006-43.
[17] T. Sjöstrand, L. Lönnblad, S. Mrenna, and P. Skands, `arXiv:hep-ph/0308153` (2003). We used version 6.323.
[18] E. E. Boos, V. E. Bunichev, L. V. Dudko, V. I. Savrin, and A. V. Sherstnev, Phys. Atom. Nucl. 69 (2006) 1317.
[19] M. L. Mangano, M. Moretti, F. Piccinini, R. Pittau, and A. D. Polosa, JHEP 07 (2003) 001.
[20] S. Höche et al., `arXiv:hep-ph/0602031` (2006).
[21] J. Pumplin et al., JHEP 07 (2002) 012.
[22] D. Stump et al., JHEP 10 (2003) 046.
[23] R. Brun and F. Carminati, CERN Program Library Long Writeup W5013 (1993).
[24] N. Kidonakis and R. Vogt, Eur. Phys. J. C 33 (2004) 466.
[25] R. Hamberg, W. L. van Neerven, and T. Matsuura, Nucl. Phys. B359 (1991) 343. Erratum-ibid. B644 (2002) 403.
[26] Z. Sullivan, Phys. Rev. D 70 (2004) 114012.
[27] J. M. Campbell and R. K. Ellis, Phys. Rev. D 60 (1999) 113006.
[28] T. Andeen et al., FERMILAB-TM-2365 (2007).
[29] I. Bertram et al., FERMILAB-TM-2104 (2000).